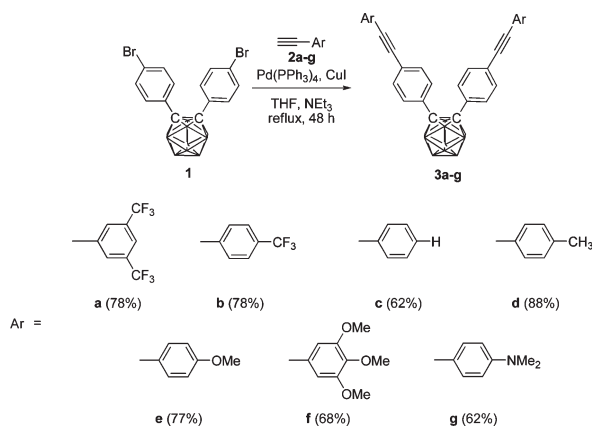


SCHEME 1. Synthetic Route for Compounds 3a–g



structure of the π -conjugated system attached to carbon atom of *o*-carborane was found to have great influence on the occurrence of the AIE property. Considering the strong electron-withdrawing property of *o*-carborane, intramolecular charge transfer from electron-donating π -conjugated units to *o*-carborane should play a key role of the observed AIE. From this point of view, we report here the design and synthesis of a series of diphenyl-*o*-carborane derivatives with electron-withdrawing and electron-donating groups in order to accomplish systematic multicolor tuning of AIE system derived from *o*-carborane.

Scheme 1 illustrates the synthetic route leading to compounds **3a–g** containing bis(4-phenylethynyl)phenyl-*o*-carborane. Bis(4-bromophenyl)-*o*-carborane **1** was synthesized from 1,2-bis(4-bromophenyl)ethyne by the addition reaction of decaborane. Then, bis(4-phenylethynyl)phenyl-*o*-carborane derivative **3a–g** was obtained via Sonogashira–Hagihara coupling reaction between **1** and arylacetylenes **2a–g**. Diphenyl-*o*-carborane derivatives **3a–g** were obtained in moderate to moderate yields after purification by flash chromatography. The structures of the obtained compounds were confirmed by ^1H , ^{13}C , and ^{11}B NMR, and high-resolution mass spectroscopies. The characteristic broaden peak at around 3.80–1.50 ppm was attributed to the presence of *o*-carborane structure. Additionally, ^{11}B NMR spectrum also showed the broad peaks at around -2.0 to -11.0 ppm, which were assigned to the boron atoms of *o*-carborane cage. This result indicates that bis(4-bromophenyl)-*o*-carborane **1** underwent the effective palladium-catalyzed reaction with various arylacetylenes.

The molecular structures of **3a**, **3c**, **3d**, and **3e** are crystallographically determined as shown in Figure 1. Three centers and two electrons bonds of *o*-carborane are perfectly retained over the palladium-coupling reaction. The bond length of C1–C2 was 1.727(5), 1.725(4), 1.725(5), and 1.736(5) Å for **3a**, **3c**, **3d**, and **3e**, respectively. As previously reported, electron-donating group in **3e** should lengthen the C1–C2

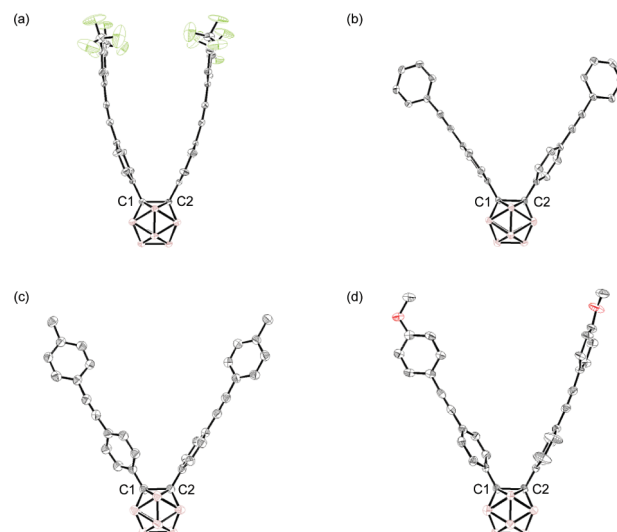


FIGURE 1. ORTEP drawings of (a) **3a**, (b) **3c**, (c) **3d**, and (d) **3e**. Thermal ellipsoids are drawn at the 50% probability level. All hydrogen atoms were omitted for clarity.

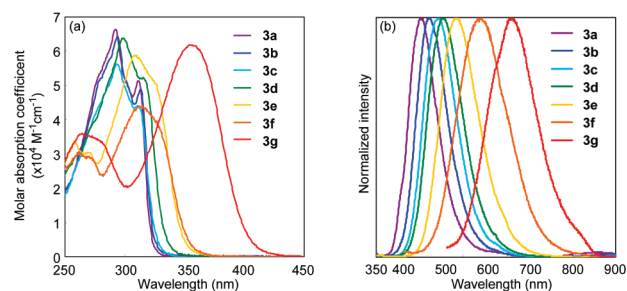


FIGURE 2. (a) UV-vis absorption spectra of **3a–g** in THF (1×10^{-5} M). (b) Photoluminescence spectra of **3a–g** in mixed solvent of THF/ H_2O = 1/99 (v/v) (1×10^{-5} M).

distance of *o*-carborane moiety, compared to the others.⁷ The crystal packing diagram of them revealed the difference of packing fashion between group A (**3a** and **3c**) and group B (**3d** and **3e**) (Figure S1, Supporting Information). Molecules in group A form dimer or double cross structure producing prismatic crystal, while those of group B form zigzag structure resulting in fibrous crystal, probably due to the position of substituent rather than its electron-withdrawing/donating ability. Indeed, compound **3b**, bearing electron-accepting trifluoromethyl units on its 4'-position, also produced a fibrous crystal (data not shown because the molecular structure was not determined).

The UV-vis absorption and photoluminescence spectra of compounds **3a–g** are shown in Figure 2 (see also Table S1, Supporting Information). The vibrational structure in the absorption spectra corresponding to $\pi \rightarrow \pi^*$ transition of diphenylacetylene moiety gradually disappeared with the increase of electron-donating ability of the substituents (**3a** \rightarrow **3g**). Further, the absorption maxima of these compounds bathochromically shifted (**3a**: 292 nm \rightarrow **3g**: 356 nm) in the same order. These facts mean that the molecule with stronger electron-donating moiety possesses greater electronic interaction between diphenylacetylene and *o*-carborane unit even in its ground state. Similarly to our previous report, compounds **3a–g** exhibited essentially no emission in the dissolved

(7) (a) Glukhov, I. V.; Antipin, M. Y.; Lyssenko, K. A. *Eur. J. Inorg. Chem.* **2004**, 7, 1379. (b) Oliva, J. M.; Allan, N. L.; Schleyer, P. v. R.; Viñas, C.; Teixidor, F. *J. Am. Chem. Soc.* **2005**, 127, 13538. (c) Llop, J.; Viñas, C.; Oliva, J. M.; Teixidor, F.; Flores, M. A.; Kivekas, R.; Sillanpää, R. *J. Organomet. Chem.* **2002**, 657, 232. (d) Llop, J.; Viñas, C.; Teixidor, F.; Victori, L.; Kivekas, R.; Sillanpää, R. *Organometallics* **2001**, 20, 4024. (e) Chupakhin, O. N.; Prokhorov, A. M.; Kozhevnikov, D. N.; Rusinov, V. L.; Kalinin, V. N.; Olshevskaya, V. A.; Glukhov, I. V.; Antipin, M. Y. *Mendelev Commun.* **2003**, 13, 165.

state.^{6a} However, these compounds started to emit intensely in the mixed solvent of THF/H₂O (1/99, Figure 2b). Substitution at the 4-position of diphenyl-*o*-carborane with electron-withdrawing and electron-donating groups strongly affected the emission spectra. The emission colors range from blue (**3a**: $\lambda_{\text{max}} = 452$ nm), to red (**3g**: $\lambda_{\text{max}} = 662$ nm) that cover almost the entire visible light, originating from aggregation induced emission (AIE). In addition, the Stokes shift of compounds **3a–g** increased with the rise of electron-donating ability of the substituents (**3a**: 140 nm \rightarrow **3g**: 306 nm). The absolute fluorescence quantum yield (Φ_F) of these compounds lies in the range of 0.10–0.31, with the exception of **3f** ($\Phi_F = 0.03$) and **3g** ($\Phi_F = 0.003$), presumably because of the charge-transfer character of the lowest energy absorption bands. These experimental observations for diphenyl-*o*-carborane derivatives confirm the expected trend in that multicolor tuning of AIE derived from *o*-carborane is accomplished by substituent variation.

To elucidate the AIE mechanism derived from *o*-carborane, we first measured the absorption and photoluminescence spectra of **3c** in a variety of solvents with different polarities (chloroform, THF, DMF, and acetonitrile). The absorption spectra of **3c** were almost invariant with identical λ_{max} value (~ 3 nm) around 294 nm, indicating that the solvent polarity has little influence on the ground state electronic transition of **3c**. On the other hand, the photoluminescence spectra of **3c** solution (a thousandth of intensity compared to that of **3c** aggregate) bathochromically shifted with increase of solvent polarity (λ_{max} : 506 nm in chloroform \rightarrow 570 nm in acetonitrile). The solvatochromic effects are usually well-described by Mataga–Lippert equation using the Stokes shifts in the different solvents (Figure 3a). $\Delta\nu$ versus Δf plot showed the linear correlation together with the large coefficient, meaning the intramolecular excited state with a larger dipolar moment than the ground state due to the substantial charge redistribution, which results from the relaxation of the initially formed Franck–Condon excited state. This result reveals that the emission process derived from *o*-carborane in dissolved state involves CT mechanism caused by electron-accepting profile of *o*-carborane.

Next, we examined the viscosity effect on the AIE of **3c**. The solution viscosity is known to restrict molecular rotations or motions which effectively annihilate the excitons.^{4d,8} As a viscous medium, we used a mixed solvent of methanol (0.55 cP) and glycerol (945 cP) with different ratios (v/v). The peak intensity of photoluminescence spectra linearly increased on single logarithm with rise of glycerol content from 0% to 75%. (Figure 3(b)), and the peak intensity of **3c** solution in the 75% glycerol/methanol mixture was 12 times higher than that in only methanol. The emission improvement in this range should result from viscosity effect, because no aggregation effect was observed when THF and water mixture was adopted.^{6a} With more than 75% of glycerol content, the aggregation effect became a leading factor of emission enhancement due to the poor solubility of **3c** in glycerol, exhibiting a similar plot to that observed in the case of mixed solution of THF and water.^{6a} This fact suggests that

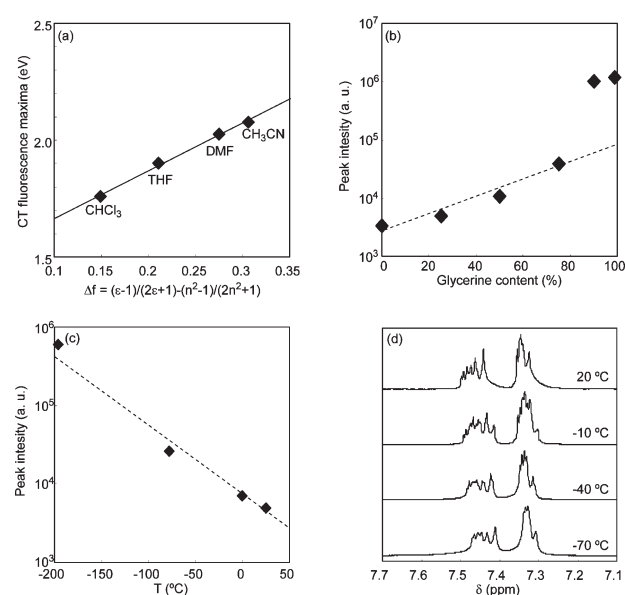


FIGURE 3. (a) Mataga–Lippert plot of **3c** measured in chloroform (CHCl₃), THF, DMF, and acetonitrile (CH₃CN) (1×10^{-5} M). (b) Photoluminescence peak intensity of **3c** vs composition of glycerol/methanol mixtures (1×10^{-5} M). (c) Effect of temperature on the peak intensity of the photoluminescence of **3c** in 2-MeTHF (1×10^{-5} M). (d) Resonance peaks of aromatic protons of **3c** in dichloromethane-*d*₂ at different temperatures.

the increase of solution viscosity effectively blocked the intramolecular motion and augmented the radiative decay.

In addition, we evaluated the temperature effect on the emission of **3c**. The emission intensity of **3c** in 2-MeTHF (1×10^{-5} M) linearly increased on semilog plot with decrease of temperature to -78 °C, giving 6-fold higher peak intensity at -78 °C compared to that at 25 °C (Figure 3c). 2-MeTHF possesses effective solvating ability with a considerably low melting point (-136 °C) and a low viscosity (1.85 cP at -70 °C), and below the melting point, it forms amorphous glass matrix.⁹ Thus, the enhancement of emission intensity upon cooling to -78 °C is predominantly caused by restricted intramolecular rotations at low temperature, rather than viscosity effect. Further decreasing of temperature from -78 to -196 °C resulted in rise of photoluminescence intensity, implying the perfect inhibition of molecular motions.

To confirm the confined molecular motions at low temperatures, variable-temperature NMR study was carried out. Until now, these studies have revealed rotation-induced conformational changes in many systems.¹⁰ Sharp resonance peaks are generally attributed to the fast conformational exchanges by rapid intramolecular motion around the single bond at room temperature, while broad peaks are observed at lower temperature due to the slowed motion. We chose deuterated dichloromethane as a solvent of **3c**, since it has a low melting point (-95 °C) and a low viscosity (0.43 cP at 20 °C) with low temperature coefficient (0.06 cP/K). As shown in Figure 3d, sharp NMR peaks were observed at room temperature, and lowering the temperature triggered broadening

(8) (a) Haidekker, M. A.; L'Heureux, N.; Frangos, J. A. *Am. J. Physiol. Heart Circ. Physiol.* **2000**, 278, H1401. (b) Haidekker, M. A.; Brady, T. P.; Chalian, S. H.; Akers, W.; Lichlyter, D.; Theodorakis, E. A. *Bioorg. Chem.* **2004**, 32, 274. (c) Förster, Th.; Hoffmann, G. *Z. Phys. Chem.* **1971**, 75, 63.

(9) Aycock, D. F. *Org. Process Res. Dev.* **2007**, 11, 156.
(10) (a) Thornberry, M. P.; Slobodnick, C.; Deck, P. A. *Organometallics* **2000**, 19, 5352. (b) Biedermann, P. U.; Stezowski, J. J.; Agranat, I. *Eur. J. Org. Chem.* **2001**, 15. (c) Wang, M.; Tang, Y.; Sato, S.; Vugmeyster, L.; McKnight, C. J.; Raleigh, D. P. *J. Am. Chem. Soc.* **2003**, 125, 6032.

of the peaks. The broadening band shape in the downfield aromatic region resulted in the coalescence of adjacent resonance peaks of protons on the benzene rings. This result verifies that the intramolecular motions in diphenyl-*o*-carborane were restricted at low temperature.

To further provide an effective understanding for the optical properties, the electronic states of **3a–g** were examined by the theoretical calculation by using the density functional theory (DFT) at the B3LYP/6-31G(d,p) level of the theory with Gaussian 03 suit program¹¹ (Table S2, Supporting Information). The calculated energy level of the highest occupied molecular orbital (HOMO) of compounds **3a–g** gradually increased from -6.61 eV (**3a**) to -5.05 eV (**3g**). Compound **3f** showed lower orbital energy of HOMO and LUMO in comparison with those of **3e**, probably due to the meta-substituted methoxy group known to have a positive substituent constant. On the other hand, **3f** experimentally exhibited red-shifted absorption and emission spectra compared to those of **3e**. The latter is consistent with the result of computed electronic transition using time-dependent DFT calculations (**3e**: $\lambda_{\text{max}} = 323$ nm, **3f**: $\lambda_{\text{max}} = 326$ nm), presumably because the electronic interaction of methoxy group in excited state should be different from that in ground state. The strong absorptions ($f > 1$) of compounds **3a–g** were mainly attributed to the transition of HOMO \rightarrow LUMO+1, and the calculated absorption maxima showed good correlation with the experimentally observed spectra. From these results, we can conclude that the substituent variation of diphenyl-*o*-carborane can systematically control the appearing color of AIE.

In summary, we report on the successful synthesis of a series of diphenyl-*o*-carborane derivatives via Sonogashira–Hagihara

palladium coupling reaction. Both electron-donating and electron-accepting arylacetylenes underwent efficient coupling reaction with bis(4-bromophenyl)-*o*-carborane, resulted in high yields. UV–vis absorption and photoluminescence spectra showed gradual bathochromic shift with the increasing of electron-donating power of the substituents. In particular, the emission spectra of these compounds cover almost the entire visible light ($\lambda_{\text{max}} = 452\text{--}662$ nm). The detailed study on AIE mechanism revealed that the restriction of molecular motions enhanced CT-based emission of *o*-carborane derivatives. Note that the theoretical calculation also demonstrated the possibility of precise color-control of aggregation-induced emission through substituent variation. Additional efforts are in progress to design other stimuli-responsive system.

Experimental Section

Synthesis of 3a. Bis(4-bromophenyl)-*o*-carborane (**1**) (454.0 mg, 1.0 mmol), bis(3,5-trifluoromethyl)phenylacetylene (**2a**, 524.0 mg, 2.2 mmol), Pd(PPh₃)₄ (58.0 mg, 0.05 mmol), and CuI (6.0 mg, 0.05 mmol) were placed in a 10 mL Pyrex tube equipped with a magnetic stirrer. The equipment was purged with Ar, followed by addition of THF (10 mL) and triethylamine (5 mL). The reaction mixture was refluxed for 48 h. After cooling, the reaction mixture was diluted with CHCl₃ and washed with aqueous NH₃ solution, water, and brine. The organic layer was dried over MgSO₄. The solvent was then removed, and the crude mixture was purified by silica gel column chromatography to afford **3a** as white powder (600 mg, 78%). ¹H NMR (400 MHz, CDCl₃): δ (ppm) 7.90 (s, 4H), 7.82 (s, 2H), 7.47 (d, 4H, $J = 8.8$ Hz), 7.35 (d, 4H, $J = 8.8$ Hz), 3.81–1.66 (br, 10H, B-H). ¹³C NMR (100 MHz, CDCl₃): δ (ppm) 132.1 (q, $J = 33.7$ Hz), 131.7, 131.4, 131.2, 130.7, 124.8, 124.2, 122.1 (q, $J = 3.9$ Hz), 121.5, 90.9, 88.7, 84.4. ¹¹B NMR (128 MHz, CDCl₃): δ (ppm) -2.2 , -9.8 . HRMS (EI): calcd for C₃₄H₂₄B₁₀F₁₂ m/z 770.2617, found 770.2608.

Acknowledgment. This study was supported by a Grant-in-Aid for JSPS Fellows (No. 09J01013) and Global COE Program “Integrated Materials Science”, MEXT, Japan.

Supporting Information Available: Experimental section, crystal packing diagram, NMR spectra, computational details, and X-ray crystallographic files (CIF). This material is available free of charge via the Internet at <http://pubs.acs.org>.

(11) Frisch, M. J.; Trucks, G. W.; Schlegel, H. B.; Scuseria, G. E.; Robb, M. A.; Cheeseman, J. R.; Montgomery, J. A., Jr.; Vreven, T.; Kudin, K. N.; Burant, J. C.; Millam, J. M.; Iyengar, S. S.; Tomasi, J.; Barone, V.; Mennucci, B.; Cossi, M.; Scalmani, G.; Rega, N.; Petersson, G. A.; Nakatsuji, H.; Hada, M.; Ehara, M.; Toyota, K.; Fukuda, R.; Hasegawa, J.; Ishida, M.; Nakajima, T.; Honda, Y.; Kitao, O.; Nakai, H.; Klene, M.; Li, X.; Knox, J. E.; Hratchian, H. P.; Cross, J. B.; Adamo, C.; Jaramillo, J.; Gomperts, R.; Stratmann, R. E.; Yazyev, O.; Austin, A. J.; Cammi, R.; Pomelli, C.; Ochterski, J. W.; Ayala, P. Y.; Morokuma, K.; Voth, G. A.; Salvador, P.; Dannenberg, J. J.; Zakrzewski, V. G.; Dapprich, S.; Daniels, A. D.; Strain, M. C.; Farkas, O.; Malick, D. K.; Rabuck, A. D.; Raghavachari, K.; Foresman, J. B.; Ortiz, J. V.; Cui, Q.; Baboul, A. G.; Clifford, S.; Cioslowski, J.; Stefanov, B. B.; Liu, G.; Liashenko, A.; Piskorz, P.; Komaromi, I.; Martin, R. L.; Fox, D. J.; Keith, T.; Al-Laham, M. A.; Peng, C. Y.; Nanayakkara, A.; Challacombe, M.; Gill, P. M. W.; Johnson, B.; Chen, W.; Wong, M. W.; Gonzalez, C.; Pople, J. A. *Gaussian 03, revision E.01*; Gaussian, Inc., Wallingford, CT, 2004.